Research Square

Preprints are preliminary reports that have not undergone peer review.
They should not be considered conclusive, used to inform clinical practice,
or referenced by the media as validated information.

Plasma Proteome Profiling of HbH-CS Disease Using TMT-Based Quantitative Proteomics Approach

yi li
First Affiliated Hospital of University of South China
Jiao Li
First Affiliated Hospital of GuangXi Medical University
Hui Chen
First Affiliated Hospital of GuangXi Medical University
Yiyun Wei
First Affiliated Hospital of GuangXi Medical University
Dong Yang
yangdong4168@163.com
First Affiliated Hospital of University of South China
Lihong Pang
First Affiliated Hospital of GuangXi Medical University

Article

Keywords: Hemoglobin H-Constant Spring disease, Proteomics, TMT labeling, NACA, Biomarker

Posted Date: September 30th, 2026

DOI: https://doi.org/10.21203/rs.3.rs-10964373/v1

License: This work is licensed under a Creative Commons Attribution 4.0 International License. Read Full License

Additional Declarations: No competing interests reported.

Abstract

Hemoglobin H-Constant Spring disease (HbH-CS) is the most clinically severe non-deletional form of α-thalassemia, yet its plasma proteomic characteristics remain unclear. In this study, we employed TMT-based quantitative proteomics to analyze differentially expressed plasma proteins between HbH-CS patients (n = 6) and healthy controls (n = 6), with validation performed in an independent cohort (45 cases per group) by ELISA. A total of 668 proteins were identified, among which 56 were differentially expressed (35 upregulated, 21 downregulated). Multivariate regression analysis identified NACA (OR = 1.014), HSP90AA1 (OR = 1.068), and PTGES3 (OR = 1.032) as independent risk factors (all P < 0.05). The area under the ROC curve (AUC) of NACA for diagnosing HbH-CS reached 0.911. NACA levels were negatively correlated with hemoglobin concentration (ρ=-0.397, P < 0.01), and the AUC for predicting severe anemia (Hb ≤ 80 g/L) was also 0.911. This study provides the first comprehensive plasma proteomic landscape of HbH-CS disease. NACA, as an independent risk factor, demonstrates excellent diagnostic efficacy and predictive value for anemia severity, and holds promise as a novel non-invasive biomarker for this disease.

1. Introduction

Thalassemia is a hereditary hemolytic anemia caused by defects in globin genes [1]. Hemoglobin H-Constant Spring disease (HbH-CS), the most common non-deletional form of α-intermediate thalassemia, results from the genotype --/α < sup > CS</sup > α and carries an increased risk of life-threatening complications [2–4]. The clinical phenotype of HbH-CS is characterized by remarkable heterogeneity: some patients become transfusion-dependent, others develop anemia only under specific physiological or pathological conditions, and some remain asymptomatic throughout life without requiring intervention. This observed dissociation between genotype and phenotype suggests that, beyond the genetic background, dynamic regulation at the proteomic level may play a critical role.

Proteomics can systematically reveal protein expression and functional changes in disease states, offering unique advantages in biomarker discovery and elucidation of disease mechanisms [5]. Today, proteomics has become one of the most important tools in biomedical research and is widely applied to study disease pathogenesis and identify biomarkers [6]. Tandem mass tag (TMT) labeling combined with liquid chromatography-tandem mass spectrometry (LC-MS/MS) enables high-throughput, high-precision relative quantification of multiple samples simultaneously, serving as a powerful tool for discovering plasma differential proteins [7].

To date, no published data exist regarding plasma protein expression differences in HbH-CS disease. Therefore, this study aims to: (1) characterize the plasma proteomic profile of HbH-CS using TMT-based quantitative proteomics; (2) identify and validate differentially expressed proteins; (3) evaluate the diagnostic efficacy of candidate biomarkers and their association with anemia severity, thereby providing potential tools for clinical stratification of HbH-CS.

2. Materials and Methods

2.1 Subjects and Sample Collection

Discovery cohort: Peripheral blood samples were collected from patients diagnosed with HbH-CS disease at the First Affiliated Hospital of Guangxi Medical University between January 2023 and November 2023 (6 cases, study group T), along with samples from 6 healthy volunteers (control group N). Inclusion criteria: (1) age 2–50 years; (2) genetically confirmed genotype --/α < sup > CS</sup > α; (3) no blood transfusion or surgical treatment within the past 3 months; (4) non-pregnant. Healthy controls were required to have no thalassemia gene carriage or other hematological diseases. Detailed clinical information is presented in **Table S1**.

Validation cohort

An expanded cohort of 45 HbH-CS patients and 45 contemporaneous healthy controls was recruited from the First Affiliated Hospital of Guangxi Medical University, Guangxi Autonomous Region People's Hospital, and Guangxi Autonomous Region Maternal and Child Health Hospital between January 2023 and July 2024, using the same inclusion criteria.

All participants or their guardians provided written informed consent. The study was approved by the Ethics Committee of the First Affiliated Hospital of Guangxi Medical University and was conducted in accordance with the Declaration of Helsinki.

The overall strategy for proteomic analysis of the discovery and validation cohorts was as follows. First, we performed TMT labeling and LC-MS/MS analysis on the discovery cohort to identify differentially expressed proteins (DEPs). Second, enzyme-linked immunosorbent assay (ELISA) was used to test the validation cohort to verify the DEPs identified in the discovery cohort. Pooled plasma samples (three biological replicates) were prepared by mixing equal volumes of two individual plasma samples from each group.

2.2 Sample Preparation

Peripheral blood (2–5 mL) was collected in EDTA-anticoagulated tubes and centrifuged at 1600×g for 15 minutes at 4°C. Plasma was separated, aliquoted, immediately snap-frozen in liquid nitrogen, and stored at -80°C until use, with repeated freeze-thaw cycles avoided.

2.3 TMT Labeling and LC-MS/MS

2.3.1 High-abundance protein depletion. Plasma samples were processed using Bio-RAD ProteoMiner beads (Catalog No. 1633007) according to the manufacturer's instructions to remove high-abundance proteins, which account for more than 80% of total plasma protein concentration. The eluate was lyophilized and reconstituted in 8 M urea.

2.3.2 Protein digestion and TMT labeling. Protein concentration was determined by the Bradford method. One hundred micrograms of protein from each sample were reduced with dithiothreitol (DTT), alkylated with iodoacetamide (IAM), and digested overnight with trypsin at an enzyme-to-protein ratio of 1:50 (w/w). After desalting, the peptides were labeled with TMT10plex reagents (Thermo Scientific) as follows: T1–T6 were labeled with 126, 127N, 127C, 128N, 128C, and 129N, respectively; N1–N6 were labeled with 129C, 130N, 130C, 131N, 131C, and 134N, respectively (**Table S2)**. The labeling reaction was carried out at room temperature for 1 hour and terminated with ammonium hydroxide.

2.3.3 High-pH fractionation and mass spectrometry analysis. The mixed labeled peptides were fractionated by high-performance liquid chromatography (HPLC) using an XBridge Peptide BEH C18 column with a gradient (0–72 minutes, 5%–95% acetonitrile) which presented in **Table S3**. Fractions were lyophilized, reconstituted, and analyzed on a Q Exactive HF-X mass spectrometer (Thermo) in data-dependent acquisition mode. The full-scan mass range was m/z 350–1800 at a resolution of 60,000 (at m/z 200). The top 15 precursor ions were selected for HCD fragmentation, and MS/MS spectra were acquired at a resolution of 45,000.

2.3.4 Database searching. Raw data were searched against the Homo sapiens UniProt database using Proteome Discoverer 2.4 software. Parameters were set as follows: enzyme, trypsin; static modification, carbamidomethyl (C); dynamic modifications, oxidation (M), TMT-16plex (K, N-term), and acetyl (protein N-term). Precursor mass tolerance was ± 15 ppm, fragment mass tolerance was ± 0.02 Da, and up to two missed cleavage sites were allowed (**Table S4**). Differentially expressed proteins were defined as those with a fold change (FC) ≥ 1.20 (upregulated) or ≤ 0.83 (downregulated) and $P < 0.05$.

2.4 Bioinformatics Analysis

Functional annotation, pathway enrichment, and protein-protein interaction network analysis were performed using COG, GO, KEGG, Reactome, and STRING databases. Subcellular localization was predicted using the ng_Locv1.0 tool.

2.5 ELISA Validation

For ten candidate differential proteins (NACA, HSP90AA1, HSP90AB1, ST13, PTGES3, NSFL1C, PGK1, HP, HPX, PRG4), commercial ELISA kits (Fankewei, China) were used to measure their concentrations in 45 pairs of plasma samples. All procedures were performed according to the manufacturer's instructions. Absorbance was measured at 450 nm, and concentrations were calculated from standard curves.

2.6 Statistical Analysis

Data were analyzed using SPSS 26.0 and GraphPad Prism 8.0. Continuous data are presented as mean ± standard deviation. Comparisons between two groups were performed using Student's t-test or Mann-Whitney U test. Categorical data were compared using the chi-square test. Correlations were assessed using Pearson or Spearman correlation analysis. Univariate and multivariate logistic regression analyses were used to identify independent risk factors. Receiver operating characteristic (ROC) curves were constructed to evaluate diagnostic performance, and the Delong test was used to compare AUC values. $P < 0.05$ was considered statistically significant (* $P < 0.05$, ** $P < 0.01$, *** $P < 0.001$).

3. Results

3.1 Clinical Characteristics and Proteomic Quality Control of the Discovery Cohort

No significant differences in age or sex were observed between the two groups in the discovery phase (**Table S5**). Bradford quantification confirmed that protein concentrations met the required standards (**Table S6**), and SDS-PAGE revealed clear bands with abundant protein profiles (**Figure S1**), confirming sample quality.

3.2 Identification of Plasma Differentially Expressed Proteins

A total of 668 proteins were identified (Fig. 1A). Among the HbH-CS-associated proteins, 35 were significantly upregulated and 21 were downregulated. Detailed information on the differentially expressed proteins (DEPs) is presented in **Table S7**. The fold change distribution, volcano plot, and hierarchical clustering heatmap of DEPs are shown in Fig. 1B,1C and 1D.

To comprehensively elucidate the biological functions of DEPs in HbH-CS, bioinformatic analyses were performed integrating COG, GO, KEGG, Pfam, and STRING databases. COG functional classification revealed that the 56 DEPs were primarily enriched in post-translational modification, protein turnover, chaperone functions, and cell cycle control (Fig. 1E). GO analysis indicated that these proteins were mainly localized to the extracellular region and cell membrane, exhibiting catalytic activity, enzyme regulatory activity, and antioxidant activity, and were involved in metabolic processes, biological regulation, and signal transduction (Fig. 1F). KEGG pathway enrichment analysis demonstrated significant involvement of DEPs in metabolic pathways, the PI3K-Akt signaling pathway, coagulation and complement cascades, MAPK and NF-κB signaling pathways, as well as the hematopoietic cell lineage, suggesting that HbH-CS involves a multi-pathway interactive network (Fig. 1G). Pfam analysis revealed enrichment of DEPs in the TCP-1/cpn60 chaperonin family, Hsp90 protein family, and AhpC/TSA antioxidant family (Fig. 1H). STRING protein-protein interaction network analysis identified NACA, HSP90AA1, HSP90AB1, HP, and HPX as central hub nodes, suggesting that these proteins may play pivotal roles in the pathological regulation of HbH-CS (Fig. 1I).

3.3 Candidate Protein Selection and ELISA Validation

To validate the proteomic findings, we quantitatively measured the top ten candidate differentially expressed proteins ranked by P-value (Table 1) in an expanded cohort of 45 paired plasma samples from patients with HbH-CS and healthy controls (N = 45, T = 45; comparative clinical data are presented in **Table S8**). ELISA results confirmed that the expression trends of all ten candidates were consistent with the proteomic data (Table 2). Among these, NACA, HSP90AA1, HSP90AB1, ST13, PTGES3, HP, and HPX exhibited significant differences between the two groups(bar graphs are shown in **Figure S2**).

Table 1
Detailed information of 10 candidate differential proteins

ID	P	log2 FC	Regulated	Description
E9PAV3	0.004	0.87588158	Up	Nascent polypeptide-associated complex subunit alpha, muscle-specific form OS=Homo sapiens OX = 9606 GN=NACA PE = 1 SV = 1
P07900	0.011	1.414867363	Up	Heat shock protein HSP 90-alpha OS=Homo sapiens OX = 9606 GN=HSP90AA1 PE = 1 SV = 5
P08238	0.018	0.856413921	Up	Heat shock protein HSP 90-beta OS=Homo sapiens OX = 9606 GN=HSP90AB1 PE = 1 SV = 4
P50502	0.008	0.926679814	Up	Hsc70-interacting protein OS=Homo sapiens OX = 9606 GN=ST13 PE = 1 SV = 2
Q15185	0.025	1.23670414	Up	Prostaglandin E synthase 3 OS=Homo sapiens OX = 9606 GN=PTGES3 PE = 1 SV = 1
Q9UNZ2	0.007	1.041873	Up	NSFL1 cofactor p47 OS=Homo sapiens OX = 9606 GN=NSFL1C PE = 1 SV = 2
P00558	0.024	-1.31427406	Down	Phosphoglycerate kinase 1 OS=Homo sapiens OX = 9606 GN=PGK1 PE = 1 SV = 3
P00738	0.028	-1.13405511	Down	Haptoglobin OS=Homo sapiens OX = 9606 GN = HP PE = 1 SV = 1
P02790	<0.001	-1.58784719	Down	Hemopexin OS=Homo sapiens OX = 9606 GN = HPX PE = 1 SV = 2
Q92954	0.003	-0.90727639	Down	Proteoglycan 4 OS=Homo sapiens OX = 9606 GN=PRG4 PE = 1 SV = 3

Table 2
Results of quantitative detection of candidate differential proteins by ELISA

Proteins	T group (n = 45)	N group (n = 45)	t	P
Up Regulated				
NACA (pg/ml)	192.20 ± 33.96	37.84 ± 8.36	4.414	< 0.001***
HSP90AA1 (pg/ml)	62.77 ± 14.21	11.13 ± 2.48	3.579	< 0.001***
HSP90AB1 (pg/ml)	97.84 ± 14.43	51.81 ± 7.81	2.806	0.006**
ST13 (pg/ml)	42.96 ± 7.52	12.74 ± 2.53	3.810	< 0.001***
PTGES3 (pg/ml)	50.83 ± 9.38	21.26 ± 5.09	2.771	0.007**
NSFL1C (pg/ml)	83.33 ± 12.27	65.03 ± 12.05	1.064	0.290
Down Regulated				
PGK1 (pg/ml)	178.30 ± 27.40	217.00 ± 42.33	0.769	0.444
HP (μg/ml)	110.20 ± 18.27	237.50 ± 31.98	3.458	< 0.001***
HPX (μg/ml)	44.17 ± 6.53	78.83 ± 10.69	2.767	0.007**
PRG4 (ng/ml)	10.64 ± 1.50	13.36 ± 1.56	1.258	0.211
*P < 0.05, **P < 0.01, ***P < 0.001.				

3.4 Correlation Analysis

Correlation analysis (Table 3) revealed significant positive correlations among NACA, HSP90AA1, HSP90AB1, ST13, and PTGES3, as well as between HP and HPX. These findings were largely consistent with the protein-protein interaction networks predicted by STRING database analysis (**Figure S3**), supporting the reliability of the identified interactions.

Table 3
Correlation analysis of candidate differential proteins

NACA	NACA	HSP90AA1	HSP90AB1	ST13	PTGES3	NSFL1C	PGK1	HP	HPX	PRG4
	1									
HSP90AA1	0.467**	1								
HSP90AB1	0.444**	0.302**	1							
ST13	0.333**	0.520**	0.375**	1						
PTGES3	0.363**	0.503**	0.259*	0.505**	1					
NSFL1C	0.211*	0.264*	0.315**	0.151	0.079	1				
PGK1	0.062	0.092	-0.039	0.061	0.015	0.091	1			
HP	-0.442**	-0.173	-0.250*	-0.236*	-0.174	-0.038	0.066	1		
HPX	-0.251*	-0.293**	-0.321**	-0.237**	-0.115	-0.063	-0.004	0.466**	1	
PRG4	-0.111	-0.123	0.081	-0.098	-0.118	0.042	0.037	0.139	0.061	1
*P < 0.05, **P < 0.01, ***P < 0.001.										

3.5 Regression Analysis and Diagnostic Performance

To identify independent factors associated with HbH-CS, we performed univariate (**Table S9**) and multivariate logistic regression analyses (Table 4). The results demonstrated that NACA, HSP90AA1, and PTGES3 were independent risk factors for HbH-CS (P < 0.05). Furthermore, receiver operating characteristic (ROC) curve analysis was conducted for the seven proteins showing statistically significant differences between groups (Fig. 2). All seven proteins—NACA, HSP90AA1, HSP90AB1, ST13, PTGES3, HP, and HPX—yielded area under the curve (AUC) values exceeding 0.70, with NACA exhibiting an AUC greater than 0.90, indicating excellent diagnostic performance.

Table 4
Multivariate logistic regression analysis

Proteins	B	OR (95%CI)	P
NACA	0.014	1.014(1.003–1.025)	0.015*
HSP90AA1	0.066	1.068(1.013–1.126)	0.015*
HSP90AB1	0.018	1.018(0.998–1.038)	0.076
ST13	0.014	1.014 (0.979–1.050)	0.439
PTGES3	0.031	1.032 (1.002–1.062)	0.033*
HP	-0.004	0.996 (0.989–1.002)	0.178
HPX	-0.022	0.978 (0.955–1.001)	0.066
*P < 0.05, **P < 0.01, ***P < 0.001.			

3.6 Correlation Between NACA and Anemia Severity

Using the median hemoglobin level of 80 g/L as the cutoff in the 45 HbH-CS patients of the validation cohort, patients were divided into severe (Hb ≤ 80 g/L, n = 23) and mild (Hb > 80 g/L, n = 22) anemia subgroups (The general clinical characteristics of these patients are detailed in **Table S10)**. Plasma NACA levels in the severe group (303.23 ± 274.75 pg/ml) were significantly higher than those in the mild group (76.17 ± 45.48 pg/ml, P < 0.001, Fig. 3A**)**. NACA levels were negatively correlated with

hemoglobin concentration (ρ = -0.397, P < 0.01, Fig. 3B). The ROC curve for predicting severe anemia showed an AUC of 0.911 (P < 0.001, Fig. 3C).

4. Discussion

This study is the first to systematically characterize the plasma proteomic landscape of HbH-CS disease using TMT-based quantitative proteomics, identifying 56 differentially expressed proteins. Through expanded cohort validation, NACA, HSP90AA1, and PTGES3 were established as independent risk factors, with NACA demonstrating both excellent diagnostic efficacy and predictive value for anemia severity. These findings provide a novel protein-level perspective for understanding the pathological mechanisms and clinical heterogeneity of HbH-CS.

Proteomic Features and Pathophysiological Associations

The molecular basis of HbH-CS is the termination codon mutation in the α2-globin gene (Constant Spring mutation), which results in reduced α-globin chain synthesis and production of an abnormally elongated α-globin variant [8–11]. Accumulation of unstable α-globin variants triggers multiple pathological effects: free β-globin chains form HbH tetramers (β4) with extremely high oxygen affinity, leading to impaired tissue oxygen delivery; oxidatively denatured α-globin chains precipitate within erythrocytes forming inclusion bodies that directly damage the membrane cytoskeleton, increase membrane permeability, and ultimately cause intravascular hemolysis [12–14].

COG analysis revealed that DEPs were enriched in functions related to post-translational modification, protein turnover, chaperones, cell cycle control, and signal transduction. Post-translational modifications play critical regulatory roles in hematopoietic development [15]. In HbH-CS, the correct folding, subunit assembly, and stability of abnormal hemoglobin may be affected by aberrant phosphorylation, glycosylation [16], and other modifications, thereby altering oxygen-binding function. Previous studies have also demonstrated abnormal post-translational modifications of proteins involved in hemoglobin assembly and erythrocyte membrane stabilization in β-thalassemia [17]. The persistent presence of abnormal hemoglobin disrupts intracellular protein homeostasis, requiring cells to accelerate abnormal protein degradation and enhance synthesis of antioxidant defense proteins [18]. Molecular chaperones play crucial roles in facilitating proper protein folding [19], but in HbH-CS, abnormal hemoglobin may interfere with chaperone function, triggering endoplasmic reticulum stress and impairing normal erythroid development. Chronic anemia stimulates compensatory bone marrow hyperplasia with accelerated proliferation of hematopoietic stem cells and erythroid progenitors [20], a process dependent on precise cell cycle regulation. The differential expression of cell cycle-related proteins observed in this study suggests that this regulatory mechanism may be compromised.

GO enrichment analysis showed that DEPs were enriched in catalytic activity, structural molecule activity, enzyme regulator activity, channel regulator activity, and antioxidant activity at the molecular function level, and in single-organism processes, biological regulation, metabolic processes, developmental processes, and signal transduction at the biological process level. The broad distribution of these functional categories reflects the multidimensional nature of HbH-CS pathophysiology. Hemoglobin synthesis and metabolism require coordinated catalysis by multiple enzymes [21]. In HbH-CS, gene mutations may alter the catalytic activity of key enzymes in related synthetic pathways, while cells adjust enzyme regulatory systems and channel activities to maintain homeostasis. The enrichment of structural molecular functions suggests that abnormal hemoglobin chain synthesis may affect the stability of erythrocyte membrane and cytoskeletal proteins, compromising erythrocyte morphology and mechanical properties. The prominent enrichment of antioxidant activity is particularly noteworthy—abnormal hemoglobin and its degradation products can induce excessive production of reactive oxygen species, requiring enhanced antioxidant defenses. Previous studies have also found that genes involved in erythropoiesis are downregulated while oxidative stress-related genes are upregulated in HbH patients [22–23], consistent with our observations. The core pathophysiology of HbH-CS involves ineffective erythropoiesis and chronic hemolysis, affecting the entire process from hematopoietic stem cell differentiation to terminal maturation, as well as iron metabolism and porphyrin metabolism pathways. The enrichment of signal transduction-related terms suggests that intercellular communication may be impaired—abnormal hemoglobin-induced erythrocyte membrane alterations may affect interactions with immune cells such as macrophages, interfering with clearance of senescent erythrocytes and contributing to the vicious cycle of hemolysis and anemia [24].

KEGG enrichment analysis revealed that DEPs were mainly involved in metabolic pathways, complement and coagulation cascades, protein processing in the endoplasmic reticulum, MAPK, NF-κB, PI3K-Akt, and hematopoietic cell lineage pathways. The complement and coagulation cascade system is maintained by coagulation factors produced by the liver and the vascular endothelium, encompassing coagulation, anticoagulation, fibrinolysis, and complement activation [25–26]. In HbH-CS, abnormal hemoglobin-induced erythrocyte membrane alterations may activate the complement system; simultaneously, procoagulant substances released from erythrocyte destruction may affect the coagulation system, leading to pathway dysregulation. The MAPK pathway is one of the core pathways regulating proliferation, differentiation, survival, and apoptosis [27–30]; the NF-κB pathway plays critical roles in inflammation and immunity [31–33]; and the PI3K-Akt pathway participates in cell growth, survival, and metabolic regulation [34]. In HbH-CS, aberrant activation or inhibition of these pathways may affect hematopoietic stem cell differentiation toward erythroid lineage, maintenance of chronic inflammatory states, and erythrocyte energy metabolism, collectively driving disease progression. The predominant subcellular localization of DEPs to the extracellular space and cytoplasm is consistent with the secretory proteins and intracellular proteins released by hemolysis reflected in the plasma proteome, further validating the reliability of our findings.

Clinical Translational Potential of NACA as a Novel Biomarker

NACA was the most prominent differential protein identified in this study. As the α subunit of the ribosome-associated chaperone NAC (nascent polypeptide-associated complex), NACA binds to the large ribosomal subunit during early protein synthesis and participates in the translocation and proper folding of nascent polypeptide chains [35]. Lopez et al. demonstrated that NACA is continuously highly expressed during erythroid differentiation of human umbilical cord blood CD34 + hematopoietic cells but is suppressed during megakaryocytic or granulocytic differentiation; overexpression of NACA accelerates erythroid differentiation and enhances hemoglobin production, while silencing NACA significantly inhibits hemoglobin synthesis [36], establishing NACA as a positive regulator of erythroid differentiation.

Our clinical data provide important complementary evidence to these findings. Plasma NACA levels in HbH-CS patients were approximately 5-fold higher than in healthy controls (192.20 vs 37.84 pg/ml). Notably, NACA levels in the severe anemia group (Hb ≤ 80 g/L) were nearly 4-fold higher than in the mild group (303.23 vs 76.17 pg/ml) and showed a significant negative correlation with hemoglobin ($\rho = -0.397$). Based on these findings, we propose the following hypothesis: in HbH-CS, α-globin synthesis deficiency leads to impaired erythropoiesis and persistent anemia, prompting the body to upregulate NACA expression through feedback regulation in an attempt to enhance erythroid progenitor differentiation and hemoglobin synthesis capacity—a compensatory protective response. However, sustained compensatory pressure may eventually exceed NACA's regulatory capacity, resulting in some patients still presenting with severe anemia. This "compensation-decompensation" dynamic balance may partially explain the phenotypic variability observed among patients with identical genotypes.

ROC analysis showed that NACA achieved an AUC of 0.911 for distinguishing HbH-CS patients from healthy controls, with the same AUC of 0.911 for predicting severe anemia. This dual high performance makes it a promising clinical application tool. In prenatal diagnosis, once an HbH-CS fetus is genetically confirmed, families face the difficult decision of whether to continue the pregnancy, yet the postnatal severity cannot be predicted—some fetuses with identical genotypes may present with only mild anemia after birth, while others may be transfusion-dependent. If NACA can be quantitatively detected in amniotic fluid or maternal peripheral blood to predict fetal phenotype, it would greatly improve the precision of genetic counseling. In disease management, dynamic monitoring of NACA may guide the timing of transfusion and intensity of iron chelation therapy, enabling personalized treatment.

HSP90AA1 and PTGES3: Components of a Synergistic Regulatory Network

HSP90AA1 and PTGES3 were also identified as independent risk factors, showing significant positive correlations with NACA, suggesting that all three may be part of the same stress-response network. HSP90AA1 encodes HSP90α, a stress-inducible cytosolic chaperone protein that plays a central role in protein quality control [37]. Its elevation in HbH-CS may reflect the cell's ongoing response to abnormal hemoglobin aggregation. PTGES3 (p23) is a co-chaperone of HSP90 and also possesses prostaglandin E synthase activity, catalyzing PGE2 synthesis [38]. PGE2 is an important signaling molecule in the hematopoietic microenvironment, regulating hematopoietic stem cell proliferation and lineage commitment. The elevation of PTGES3 may serve two purposes simultaneously: cooperating with HSP90 to process misfolded proteins, while promoting erythroid progenitor

expansion through PGE2 signaling. The strong correlation of NACA with both proteins suggests the existence of a coordinated regulatory axis comprising "stress sensing–protein quality control–erythroid differentiation promotion," warranting further mechanistic investigation.

Clinical Significance and Limitations

The strengths of this study include the use of high-precision TMT quantification and expanded cohort validation, providing the first comprehensive proteomic characterization of HbH-CS. Limitations include: (1) relatively small sample size in the discovery phase, though this was partially mitigated by the validation cohort (45 cases per group) and statistical robustness; (2) cross-sectional design precluding tracking of dynamic NACA changes and their relationship with clinical events; and (3) lack of inclusion of other thalassemia genotypes as controls, requiring further validation of NACA specificity.Future prospective multicenter cohort studies are needed to evaluate the practical value of NACA in prenatal diagnosis and prognostic stratification, and to explore its potential as a therapeutic target.

5. Conclusion

This study provides the first comprehensive plasma proteomic landscape of HbH-CS disease, revealing systemic involvement of complement/coagulation, protein processing, and oxidative stress pathways. NACA was identified as a novel biomarker with excellent diagnostic efficacy and predictive value for anemia severity, with its upregulation potentially representing a compensatory erythroid differentiation response to anemia. HSP90AA1 and PTGES3, as independent risk factors, form a potential synergistic regulatory network with NACA. These findings not only deepen our understanding of the pathological mechanisms of HbH-CS but also provide proteomics-based translational tools for prenatal risk assessment and clinical stratification management of this disease.

Declarations

Competing interests

The authors declare that the research was conducted in the absence of any commercial or financial relationships that could be construed as a potential conflict of interest.

Ethics approval and consent to participate

All study procedures follow the principles of the Declaration of Helsinki. Ethical approval for this study was obtained from the First Affiliated Hospital of Guangxi Medical University. The approval number is 2023-NK-Gui Kegong-001. All patients included in the study have signed informed consent forms.

Patient consent statement

All patients included in the study have signed informed consent forms. Written informed consent was obtained from a legally authorized representative(s) for anonymized patient information to be published in this article.

Consent for publication

Not applicable.

Competing interests

The authors declare that the research was conducted in the absence of any commercial or financial relationships that could be construed as a potential conflict of interest.

Supporting Information

supporting information can be found online in the Supporting Information section. **Figure S1**: Results of SDS-PAGE electrophoresis. **Figure S2**: Quantitative analysis of 10 candidate differential proteins by ELISA(A: NACA;B□HSP90AA1□C□HSP90AB1□D□ST13□E□PTGES3□F□NSFL1C□G□PGK1□H□HP□I□HPX□J□PRG4. * P < 0.05, **P < 0.01, ***P < 0.001.) **Figure S3**: Interaction network diagram of 10 candidate differential proteins. **Table S1**: clinical information of participants. **Table S2**: Isotope labeling design table. **Table S3**: Separation gradient of fractionation treatment. **Table S4**: Search database retrieval parameter Settings. **Table S5**: Comparison of general information between the two groups. **Table S6**: Quantitative results of protein. **Table S7**: Details of differential proteins. **Table S8**: Comparison of clinical data between the two groups. **Table S9**: Univariate analysis. **Table S10**: Comparison of clinical data in subgroup analysis.

Funding information

This work was supported by grants from the National Natural Science Foundation of China (Nos. 81960281;82260306); Clinical Research Climbing Program of the First Affiliated Hospital of Guangxi Medical University (No. YYZS2022006)□the construction of clinical intervention protocols Guangxi key R & D program(Guike AB20159031; AB24010080)□the Natural Science Foundation of Hunan Province (Grant Number 2026JJ80198) and the Doctoral Startup Fund of the First Affiliated Hospital of University of South China.

Author Contribution

Y.L., J.L., H.C. and Y. Y.W. performed the experiments, collected and analyzed the data. Y.L. and J.L. conducted the bioinformatics and statistical analyses. Y.L. designed the study and drafted the manuscript. D.Y. and L.H.P. conceived the study, supervised the project, critically revised the manuscript for important intellectual content, and provided administrative and funding support. All authors contributed to the inclusion of patients and recording of data, critically reviewed the manuscript, and gave final approval for publication. They agree to be accountable for all aspects of the work. The corresponding authors attest that all listed authors meet the authorship criteria and that no others meeting the criteria have been omitted. D.Y. and L.H.P. are the guarantors.

Acknowledgement

We are grateful for the support and help from the Key Laboratory of Early Prevention and Treatment for Regional High-Frequency Tumors (Gaungxi Medical University), Ministry of Education, Nanning, Guangxi, China. The views expressed in this article are the personal opinions of the authors and do not reflect the policy of the Department of Health and Human Services Funding. TMT-tagged quantitative proteomics were performed by BestMS Technologies Co., LTD(Qingdao, China)(http://www.bestms.cn/).

Data Availability

The datasets used and/or analysed during the current study are available from the corresponding author on reasonable request.

References

1. Wu, X. D., Xu, X. X. & Zhu, Y. P. Classification and diagnostic criteria for thalassemia. *Chin. J. Pract. Pediatr.* **33** (12), 957–961 (2018).
2. Chui, D. H. K., Fucharoen, S. & Chan, V. Hemoglobin H disease: not necessarily a benign disorder. *Blood* **101**, 791–800 (2003).

3. Fucharoen, S., Viprakasit, V. & Hb, H. disease: clinical course and disease modifiers. *Hematol. Am. Soc. Hematol. Educ. Program.* :26–34. (2009).
4. Lal, A. et al. Heterogeneity of hemoglobin H disease in childhood. *N Engl. J. Med.* **364** (8), 710–718 (2011).
5. Cheng, N. *Potential diagnostic biomarkers in plasma for acute aortic dissection based on iTRAQ proteomics technology [D]* (Xinjiang Medical University, 2023).
6. Rozanova, S. et al. Quantitative Mass Spectrometry-Based Proteomics: An Overview. *Methods Mol. Biol.* **2228**, 85–116 (2021).
7. Gabriel, W. et al. Prosit-TMT: Deep Learning Boosts Identification of TMT-Labeled Peptides. *Anal. Chem.* **94** (20), 7181–7190 (2022).
8. Thein, S. L. Molecular Basis of β Thalassemia and Potential Therapeutic Targets. *Blood Cells Mol. Dis.* **70**, 54–65 (2018).
9. Traxler, E. A. et al. A Genome-Editing Strategy to Treat β-Hemoglobinopathies That Recapitulates a Mutation Associated With a Benign Genetic Condition. *Nat. Med.* **22** (9), 987–990 (2016).
10. Aldemir, Ö. The Genetic Aspect of Thalassemia: From Diagnosis to Treatment. In: Thalassemia and Other Hemolytic Anemias. London: IntechOpen; (2018).
11. Farashi, S. & Harteveld, C. L. Molecular Basis of α-Thalassemia. *Blood Cells Mol. Dis.* **70**, 43–53 (2018).
12. Patsali, P. et al. Short-Hairpin RNA Against α-Globin (HbA-sh3) for the Treatment of β-Thalassemia: In Vitro and In Vivo Validation Studies. *Haematologica* **103** (9), e403–e407 (2018).
13. Taher, A. T., Weatherall, D. J., Cappellini, M. D. & Thalassaemia *Lancet* ;**391**(10116):155–167. (2018).
14. Ramli, M. et al. Significance of Zone 2 Peak on Capillary Electrophoresis in the Detection of Hemoglobin Constant Spring. *Oman Med. J.* **38** (3), e507 (2023).
15. Wang, D. *Mechanistic study of alternative splicing events and SETD7-mediated post-translational modification events in hematopoietic development [D]* (Peking Union Medical College, 2023).
16. Conradi, C. & Shiu, A. Dynamics of posttranslational modification systems: recent progress and future directions. *Biophys. J.* **114** (3), 507–515 (2018).
17. Gong, Y. et al. A natural DNMT1 mutation elevates the fetal hemoglobin level via epigenetic derepression of the γ-globin gene in β-thalassemia. *Blood* **137** (12), 1652–1657 (2021).
18. Wang, L. et al. Oxidative stress status and its regulation of hepcidin in HbH-CS patients. *Chin. J. Exp. Hematol.* **26** (5), 1465–1470 (2018).
19. Piplani, B. et al. Mycobacterial chaperonins in cellular proteostasis: Evidence for chaperone function of Cpn60.1 and Cpn60.2-mediated protein folding. *Mol. Microbiol.* **120** (2), 210–223 (2023).
20. Lal, A. et al. Disease burden, management strategies, and unmet needs in α-thalassemia due to hemoglobin H disease. *Am. J. Hematol.* **99** (11), 2164–2177 (2024).
21. Li, X. H., Sun, J. H. & Sun, J. G. Advances in cyclin-dependent kinase family research. *Prog Pharm. Sci.* **49** (1), 60–68 (2025).
22. Dickerhoff, R. Non-Transfusion-Dependent Thalassemia (NTDT)—Therapy. *Oncol. Res. Treat.* **39** (Suppl 3), 41–44 (2016).
23. Dupont, J. B. Genetic Diseases in the Omics Era. *Mol. Ther.* **29** (8), 2577–2578 (2021).
24. Ningtyas, D. C. et al. Platelets mediate the clearance of senescent red blood cells by forming prophagocytic platelet-cell complexes. *Blood* **143** (6), 535–547 (2024).
25. Xia, D. Clinical significance of prothrombin time and platelet parameters in patients with liver cirrhosis. *Pract. Lab. Med. J.* **10** (3), 179–181 (2018).
26. Chen, J. et al. Changes in coagulation factors and their relationship with coagulation status in patients with different types of liver disease. *Chin. J. Hepatol.* **20** (3), 206–210 (2012).
27. Wang, Q. et al. Unveiling the role of tRNA-derived small RNAs in MAPK signaling pathway: implications for cancer and beyond. *Front. Genet.* **15**, 1346852 (2024).
28. Cheng, Y. et al. Virus-induced p38 MAPK activation facilitates viral infection. *Theranostics* **10** (26), 12223–12240 (2020).

29. Qin, M. Y. et al. Drug-containing serum of rhubarb-astragalus capsule inhibits the epithelial-mesenchymal transformation of HK-2 by downregulating TGF-β1/p38MAPK/Smad2/3 pathway. *J. Ethnopharmacol.* **280**, 114414 (2021).
30. Reschke, L. et al. Leptin induces leiomyoma cell proliferation and extracellular matrix deposition via JAK2/STAT3 and MAPK/ERK pathways. *F S Sci.* **3** (4), 383–391 (2022).
31. Sun, Y. et al. Artificial intelligence defines protein-based classification of thyroid nodules. *Cell. Discov*. **8** (1), 85 (2022).
32. Guo, Y. et al. Multiplex cerebrospinal fluid proteomics identifies biomarkers for diagnosis and prediction of Alzheimer's disease. *Nat. Hum. Behav.* **8** (10), 2047–2066 (2024).
33. Feng, R. et al. Activation of γ-globin expression by hypoxia-inducible factor 1α. *Nature* **610** (7933), 783–790 (2022).
34. Lou, R. et al. Benchmarking commonly used software suites and analysis workflows for DIA proteomics and phosphoproteomics. *Nat. Commun.* **14** (1), 94 (2023).
35. Song, D. et al. The ribosomal chaperone NACA recruits PHD2 to cotranslationally modify HIF-α. *EMBO J.* **41** (22), e112059 (2022).
36. Lopez, S. et al. NACA is a positive regulator of human erythroid-cell differentiation. *J. Cell. Sci.* **118** (Pt 8), 1595–1605 (2005).
37. Noddings, C. M. et al. Structure of Hsp90-p23-GR reveals the Hsp90 client-remodelling mechanism. *Nature* **601** (7893), 465–469 (2022).
38. Zhao, J. et al. Targeting PGE2 mediated senescent neuron improves tumour therapy. *Neuro Oncol.* (2025).

Figures

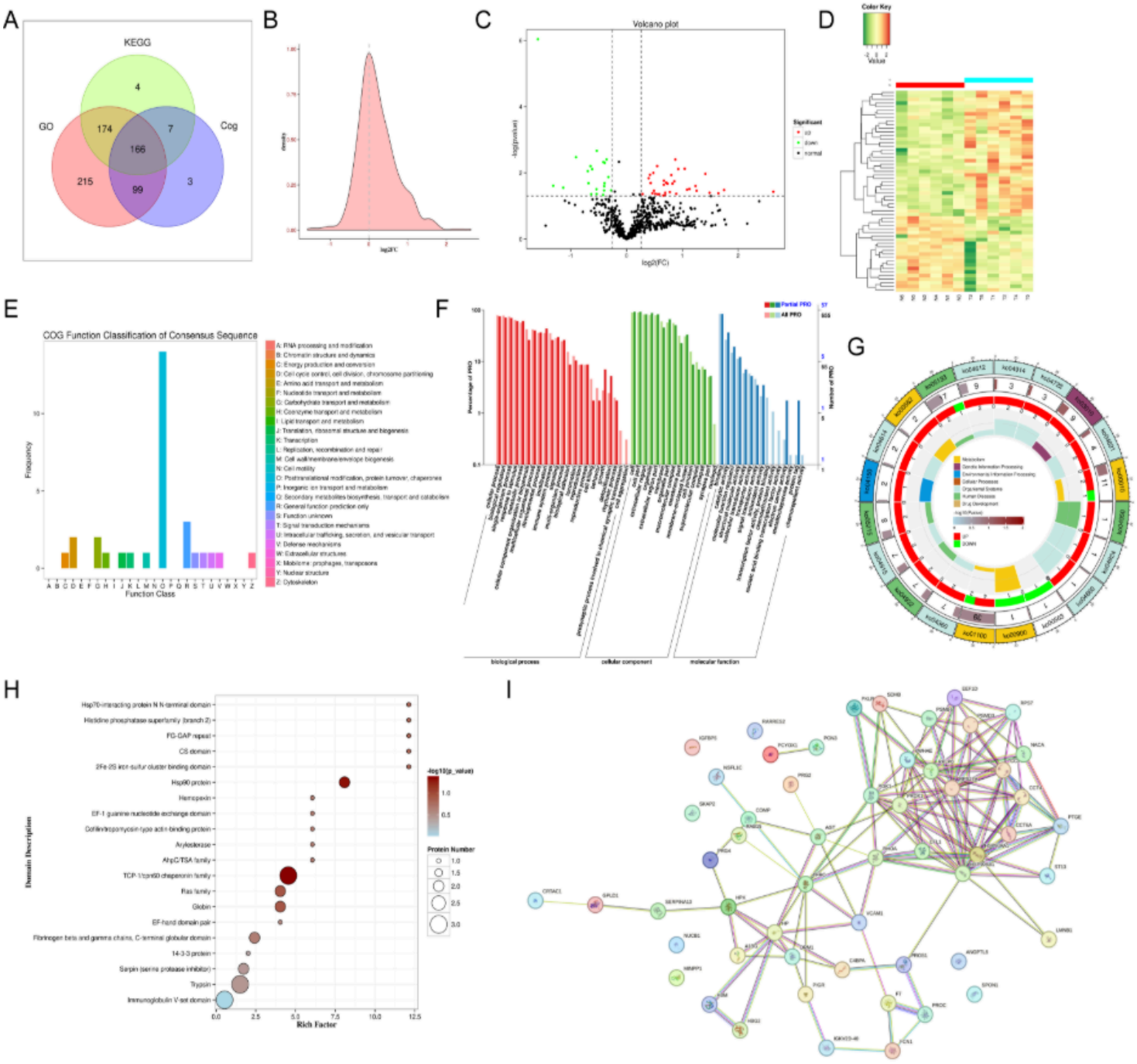


Figure 1

TMT proteomics results for 6 sample groups.

(A) Venn diagram; (B) Distribution of differential protein multiples; (C) Volcano plot; (D) Clustering heatmap; (E) COG annotation; (F) GO annotation; (G) KEGG enrichment; (H) Pfam enrichment; (I) STRING interaction network.

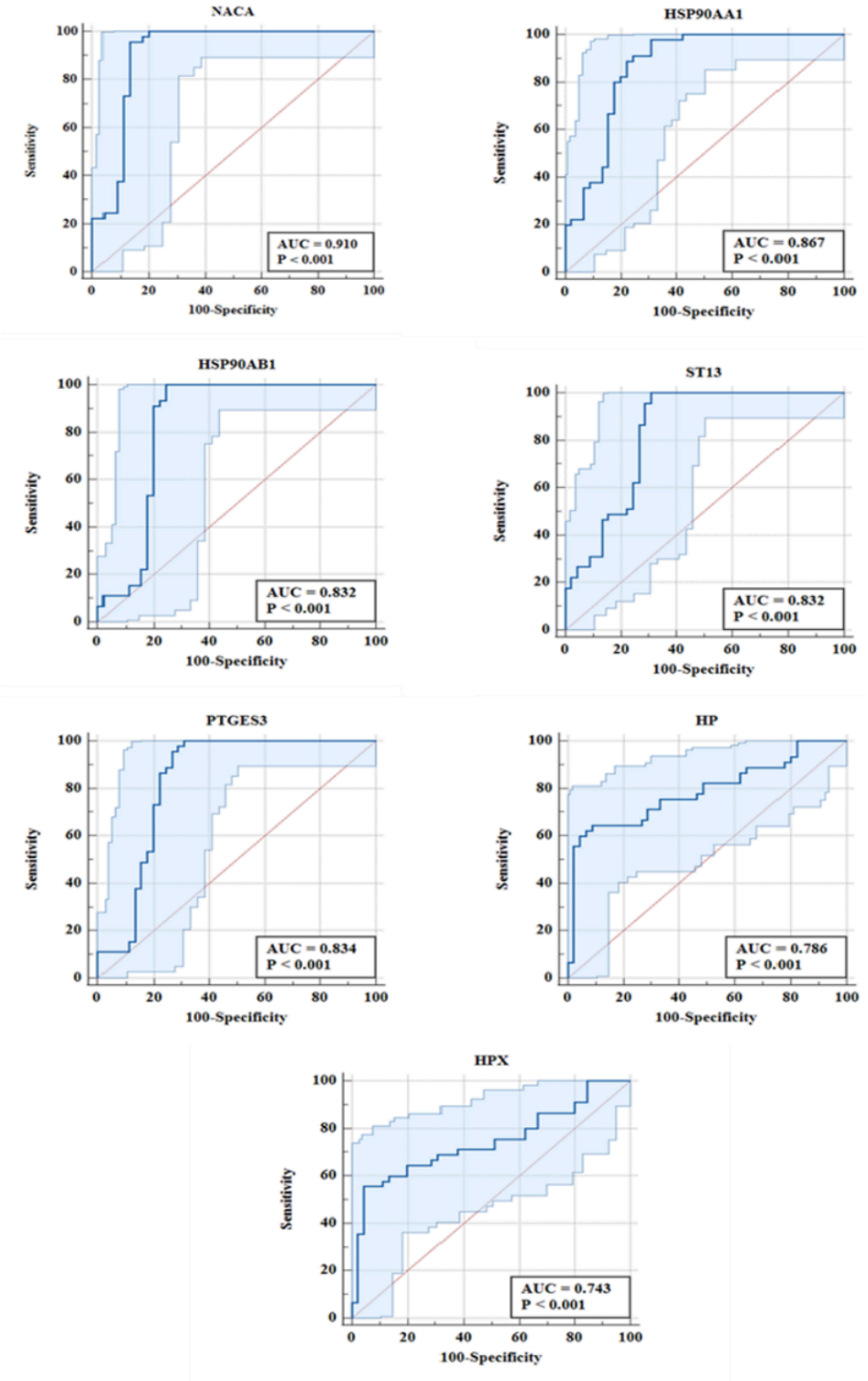


Figure 2

ROC curves of candidate differential proteins

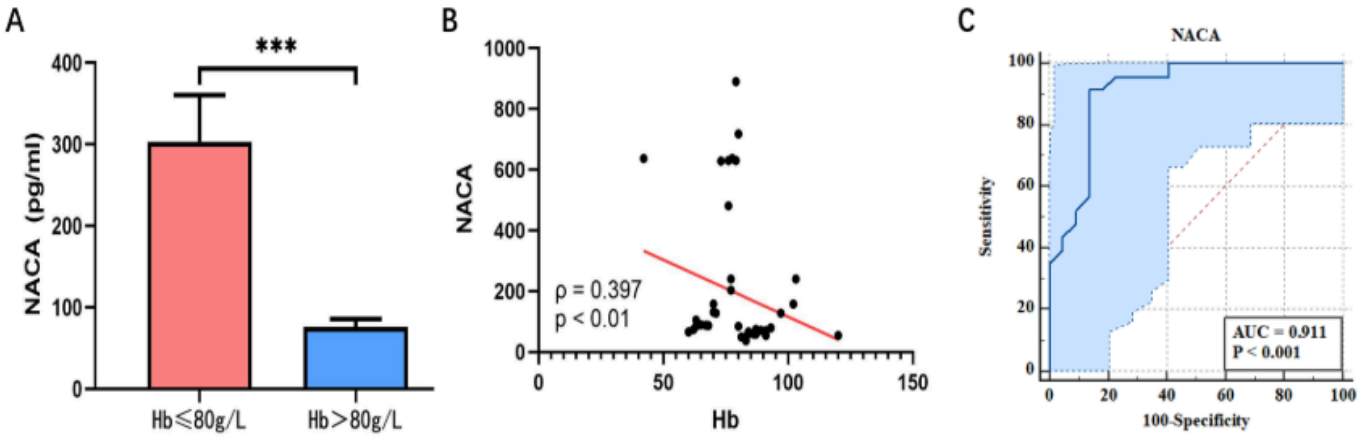


Figure 3

Analysis of NACA in subgroups. (A) Comparison of NACA protein in subgroups; (B) correlation analysis between NACA and hemoglobin level; (C) NACA ROC curve analysis. **P<0.01, ***P<0.001.

Supplementary Files

This is a list of supplementary files associated with this preprint. Click to download.

- Supplementaryfigureandtable8.5.docx